

## Corrosion characterization of the experimental alloy Ti-35Nb-7Zr-5Ta by electrochemical techniques

Caracterização da corrosão da liga experimental Ti-35Nb-7Zr-5Ta por técnicas eletroquímicas

Caracterización de la corrosión de la aleación experimental Ti-35Nb-7Zr-5Ta mediante técnicas electroquímicas

Received: 05/07/2021 | Reviewed: 05/14/2021 | Accept: 05/17/2021 | Published: 06/04/2021

**Ana Elisa Vilicev Italiano**

ORCID: <https://orcid.org/0000-0003-4714-8478>  
São Paulo State University, Brazil  
E-mail: [anevitaly@gmail.com](mailto:anevitaly@gmail.com)

**Daniela Vieira Amantéa**

ORCID: <https://orcid.org/0000-0001-6749-2634>  
São Paulo Anhanguera University, Brazil  
E-mail: [dvamantea1974@gmail.com](mailto:dvamantea1974@gmail.com)

**Fernando Santos da Silva**

ORCID: <https://orcid.org/0000-0003-0606-6126>  
São Paulo State University, Brazil  
E-mail: [ferdekfernando@gmail.com](mailto:ferdekfernando@gmail.com)

**Leandro Fernandes**

ORCID: <https://orcid.org/0000-0003-0384-3604>  
São Paulo State University, Brazil  
E-mail: [leanfernandes@alumni.usp.br](mailto:leanfernandes@alumni.usp.br)

**Márcio Luiz dos Santos**

ORCID: <https://orcid.org/0000-0002-6607-1640>  
São Paulo Anhanguera University, Brazil  
E-mail: [marcio.l.santos@educadores.net.br](mailto:marcio.l.santos@educadores.net.br)

**Luís Geraldo Vaz**

ORCID: <https://orcid.org/0000-0003-0916-1962>  
São Paulo State University, Brazil  
E-mail: [lugervaz@foar.unesp.br](mailto:lugervaz@foar.unesp.br)

### Abstract

The objective of the present study was to evaluate the corrosion resistance of the experimental alloy Ti-35Nb-7Zr-5Ta, modified by laser beam, in a physiological solution of 0.9% NaCl. This evaluation was carried out by open circuit potential analysis ( $E_{OCP}$ ), potentiodynamic polarization curves and cyclic polarization curves. The open circuit potential curves show the specimen irradiated by laser beam at 35 Hz presented a more stable and corrosion resistant surface. It was observed in the polarization curves, low current densities in the order of nA/cm<sup>2</sup>, for all specimen indicating an expected passive behavior for the investigated alloy. The cyclic polarization curves show that for specimen treated with laser, the potential for repassivation ( $E_r$ ) is greater in relation to the potential for corrosion ( $E_{corr}$ ), which indicates greater resistance to corrosion of metal alloys when treated with laser.

**Keywords:** Titanium alloys; Biomaterials; Electrochemical techniques; Corrosion; Osseointegration.

### Resumo

O objetivo do presente estudo foi avaliar a resistência à corrosão da liga experimental Ti-35Nb-7Zr-5Ta, modificada por feixe de laser, em uma solução fisiológica de NaCl a 0,9%. Esta avaliação foi realizada por análise de potencial de circuito aberto ( $E_{OCP}$ ), curvas de polarização potenciodinâmica e curvas de polarização cíclica. As curvas de potencial de circuito aberto mostram que a amostra irradiada por feixe de laser a 35 Hz apresentou uma superfície mais estável e resistente a corrosão. Observou-se nas curvas de polarização, baixas densidades de corrente na ordem de nA/cm<sup>2</sup>, para todas as amostras indicando um comportamento passivo esperado para a liga investigada. As curvas de polarização cíclica mostram que para as amostras tratadas a laser o potencial de repassivação ( $E_r$ ) é maior em relação ao potencial de corrosão ( $E_{corr}$ ), o que indica uma maior resistência a corrosão das ligas metálicas quando tratadas a laser.

**Palavras-chave:** Ligas de titânio; Biomateriais; Técnicas eletroquímicas; Corrosão; Osseointegração.

## Resumen

El objetivo del presente estudio fue evaluar la resistencia a la corrosión de la aleación experimental. Ti-35Nb-7Zr-5Ta, modificado por rayo láser, en una solución fisiológica de NaCl al 0,9%. Esta evaluación se llevó a cabo mediante análisis de potencial de circuito abierto ( $E_{OCP}$ ), curvas de polarización potenciodinámica y curvas de polarización cíclica. Las curvas de potencial de circuito abierto muestran que la muestra irradiada por rayo láser a 35 Hz presentó una superficie más estable y resistente a la corrosión. Se observó en las curvas de polarización, densidades de corriente bajas del orden de  $nA/cm^2$ , para todas las muestras indicando un comportamiento pasivo esperado para la aleación investigada. Las curvas de polarización cíclica muestran que para las muestras tratadas con láser, el potencial de repasivación ( $E_r$ ) es mayor en relación al potencial de corrosión ( $E_{corr}$ ), lo que indica una mayor resistencia a la corrosión de las aleaciones metálicas cuando se tratan con láser.

**Palabras clave:** Aleaciones de titanio; Biomateriales; Técnicas electroquímicas; Corrosión; Osteointegración.

## 1. Introduction

For dental and orthopedic applications, titanium has a successful history for use in biomaterials due to its biocompatibility. With a highly active oxide layer, this material is very well accepted by local fabrics. (Mish, 2000; Santos et al., 2007) Titanium alloys have numerous properties are suitable for such applications as, high resistance to corrosion, biocompatibility, and low specific weight. (Kuroda et al., 1998; Niinomi, et al 1999; Rodrigues et al., 2015)

Considering the metallic components used in implantable devices are constantly subjected to aggressive means, the study corrosion is fundamental importance for the understanding its performance and functionality, when applied clinically.(Lopes et al., 2016; Paital & Dahotre, 2009) Corrosion resistance is evaluated as a vital property for these applications, considering corrosion products are responsible for biocompatibility, since they can produce undesirable reactions to the organism.(De Assis et al., 2006; Trivinho-Strixino, F; Santos, J S; Sikora, 2017) Studies carried out by Chai et al and Lopez et al, showed the development of new low-toxicity, vanadium-free Ti-based alloys, such as Ti-7Nb-6Al, Ti-13Nb-13Zr and Ti-15Zr-4Nb, for use as biomaterials, demonstrating the spontaneous formation an oxide layer in contact with air.(Chai et al., 2008; López et al., 2001)

The modification the surface can promote improvement the corrosion resistance the material, increase of the bioactivity characteristic of the titanium oxides formed spontaneously on the surface, presenting promising results in the interaction with the tissue, since the biocompatibility (inertiality or bioactivity) is determined by chemical processes occur at the interface between the prosthesis and the living tissue.(Capellato, 2020; Chen et al., 2013; Geetha et al., 2009; Mohammed et al., 2015; Rungsiyakull et al., 2010) One of the most promising surface modifications is laser beam irradiation, a technique that consists of providing a large irregularity on the surface the material in a " clean " manner to create a morphology with a large specific area and physical properties-chemicals suitable for promoting the interaction of apatites and providing the formation of a great diversity of oxides aiming induce the phenomenon of osseointegration more effectively and satisfactorily.(Queiroz et al., 2013; Valente, 2017) Some researchers, in a study using Nd; YAG lasers, found that implants with surfaces modified by laser beam, present better and more stable fixation to the bone in relation to the machined ones, and attributes this characteristic to the oxidation process of the surface contributing to a favorable way for the osseointegration process, providing increased hardness and corrosion resistance, as well as improved wettability and increased free surface energy.(Filho et al., 2011; Laurindo, Lepiensi, Amorim, Torres, Soares, 2018)

In this research, we sought to elucidate the corrosion resistance of the Ti-35Nb-7Zr-5Ta alloy and evaluate the film formed on the surface before and after modification by laser beam, using the following electrochemical techniques: open circuit potential (OCP), potentiodynamic polarization and cyclic polarization.

## 2. Methodology

Specimen the  $\beta$  Ti-35Nb-7Zr-5Ta alloy (% m / m) were obtained by the authors from the methodology of previous studies (P. A. B. Kuroda & Nascimento, M V; Grandini, 2020; Miotto et al., 2016) using an arc melting furnace under an ultra-pure argon atmosphere, obtaining ingots approximately 10 cm long and 1 cm thick which then underwent heat treatment at 1000°C for 8 hours and slow air cooling, to remove internal stresses from the casting process. Then they were machined and cut to dimensions of 8.0 mm in diameter and 2.0 mm in thickness and separated into groups: specimen without surface modification, specimen with a laser irradiated surface at 20 Hz and specimen with an irradiated surface at 35Hz laser. The specimen was mechanically polished with 320 to 2000 mesh granulation sandpaper and was subjected to a process of immersion in isopropyl alcohol and distilled water, in that order, in ultrasound equipment, lasting 30 minutes each. Then the polishing was carried out in an electric polisher (Arotec, Aropol 2V), with cloth soaked in 0.5  $\mu$ m granulation alumina and again were immersed in isopropyl alcohol and distilled water, in ultrasound equipment, for 30 minutes each. The surface modification was performed using Yb: YAG laser beam irradiation, in the parameters mentioned in Table 1. The cleaning of the specimen after laser beam irradiation was done with isopropyl alcohol, acetone, and distilled water, respectively in equipment ultrasound for 10 minutes.

**Table 1** - Parameters used for laser irradiation in the Ti-35Nb-7Zr-5Ta alloy.

LASER PROPERTY	PARAMETERS
Beam power (W)	maximum
Scanning speed (mm / s)	100
Space between scans (mm)	0.01
Pulse frequency (Hz)	20 -35
Average exposure area (mm)	0.8

Source: Survey data.

The electrochemical experiments were conducted in accordance with the provisions of the literature.(De Assis et al., 2006; Rodrigues et al., 2015; Varella Rodrigues & Carlos Guastaldi, 2018) In a standard cell of three electrodes with an exposed area of 0.8 cm<sup>2</sup> of working electrode, with a platinum mesh as a counter electrode and silver / silver chloride (Ag / AgCl<sub>sat</sub>) as the reference electrode. These studies were carried out in a 0.9% NaCl solution, at room temperature, in media and conditions simulate the aggressiveness of human body fluids. The open circuit potential ( $E_{ocp}$ ) was measured during the time of  $\approx$  20 h until its variation with time became negligible. The potentiodynamic and cyclic polarization tests were performed immediately after 20h of immersion, without removing the specimen from the electrochemical cell and without changing the solution. For the potentiodynamic polarization measures, an initial potential  $E_1 = - 0.1V$  vs. (Ag / AgCl<sub>sat</sub>) was used up to  $E_2 = 2V$  vs. (Ag / AgCl<sub>sat</sub>) and scan speed of 5 mV / s. For cyclic polarization measurements, the initial potential was  $E_1 = - 0.5 V$  vs. (Ag / AgCl<sub>sat</sub>) with  $E_2$  reversal potential = 1.5 V vs. (Ag / AgCl<sub>sat</sub>) and final potential of  $E_1 = - 1 V$  vs. (Ag / AgCl<sub>sat</sub>), with scanning speed of 5 mV / s.

## 3. Results

### 3.1 Open Circuit Potential ( $E_{ocp}$ )

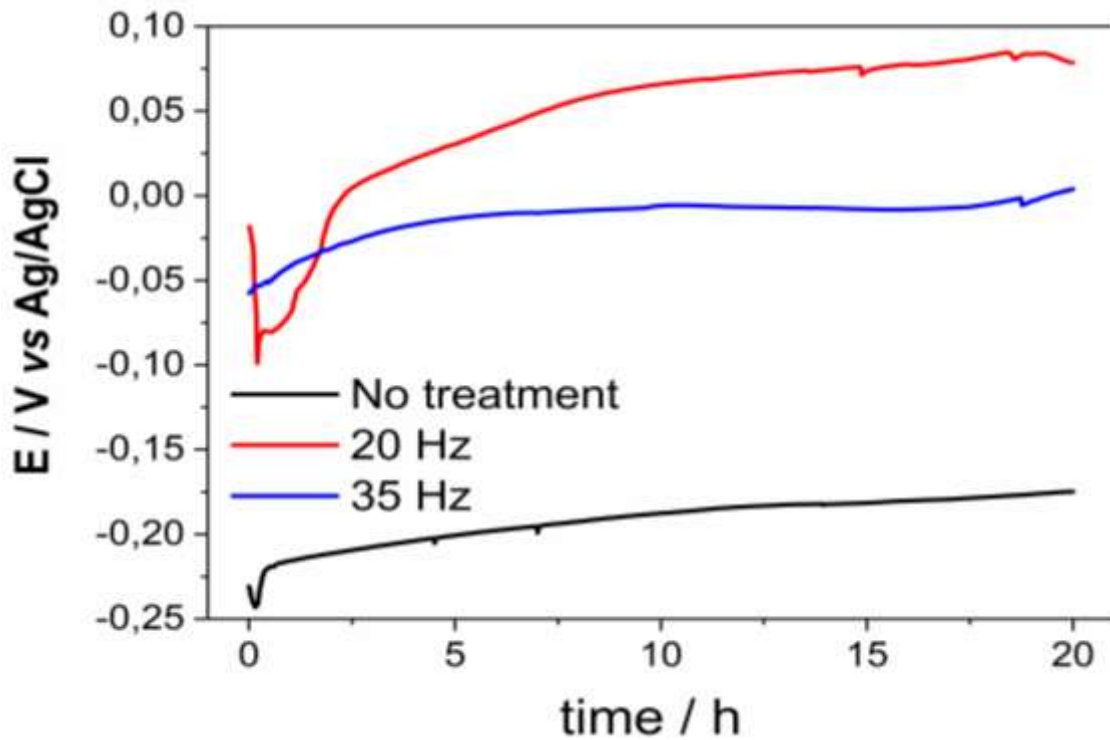
Corrosion resistance of metallic materials can be assessed by simple  $E_{ocp}$  measurements. Under conditions of open circuit potential, cathodic and anodic electrochemical reactions are simultaneous and occur spontaneously.(Silva et al., 2017)

The monitoring of this spontaneous process allows to measure the potential variation over time and to verify the formation or dissolution behavior of oxide films on the surface of metals or metal alloys. (Rodrigues et al., 2015)

Figure 1 shows the curves obtained for the variation of  $E_{ocp}$  versus time for Ti-35Nb-7Zr-5Ta in the three proposed conditions, in 0.9% NaCl solution during 20 hours of analysis. It is observed in the untreated specimen - there is initially a decrease in the open circuit potential attributed to the dissolution of the native oxide layer on the alloy surface, adsorption of chloride ions, dissolution of alloy elements and changes in ion concentrations on the surface and oxygen. (Silva et al., 2017) After 20 min the  $E_{ocp}$  value starts to rise, due to the formation of a passive layer of titanium oxide. The growth of the titanium oxide layer is slow and acts to protect the surface of the material, which can be confirmed by the gradual increase in the value of the  $E_{ocp}$ . After 20 h of immersion, the  $E_{ocp}$  value stabilizes at -0.17 V (Ag / AgCl<sub>sat</sub>).

For the 20 Hz laser treated specimen, the  $E_{ocp}$  value is -0.05 V (Ag / AgCl<sub>sat</sub>) at the beginning of the experiments. After a few minutes there is a sudden decrease in the value of the open circuit potential reaching -0.10 V (Ag / AgCl<sub>sat</sub>) with a time of 30 minutes. This decrease can be attributed two process: the diffusion of electrolytes through defects of the passive film and pores in the oxide layers until it reaches the surface of the metal alloy, starting its corrosion and attack of chloride ions on the surface of the metal alloy. After 30 min the potential begins to increase due to the formation of a stable layer of metallic oxides on the surface of the alloy, mainly in the anodic areas. After about 10 h the  $E_{ocp}$  value remains practically constant, although it is possible to observe some potential fluctuations can be attributed to the passivation and repassivation process of the protective oxide layer. The specimens treated with laser at 35 Hz showed an increase in the  $E_{ocp}$  value from the beginning of the tests until approximately 10 h of immersion. After this time, a stabilization in the  $E_{ocp}$  value can be observed. This behavior shows the oxide layer formed after laser treatment has the characteristic of being more dense, uniform, and compact, since it is electrochemically stable and does not allow the electrolyte to reach the surface of the metal alloy causing oscillations in the potential values. This type of behavior, in which there is an increase in potential as soon as the metallic material is exposed to the electrolyte, is typical of systems present the formation of a thick film.

**Figure 1** - Values of open circuit potential versus time for Ti-35Nb7Zr-5Ta in 0.9% NaCl solution, in conditions without surface treatment and with laser beam irradiation at 20Hz and 35Hz.



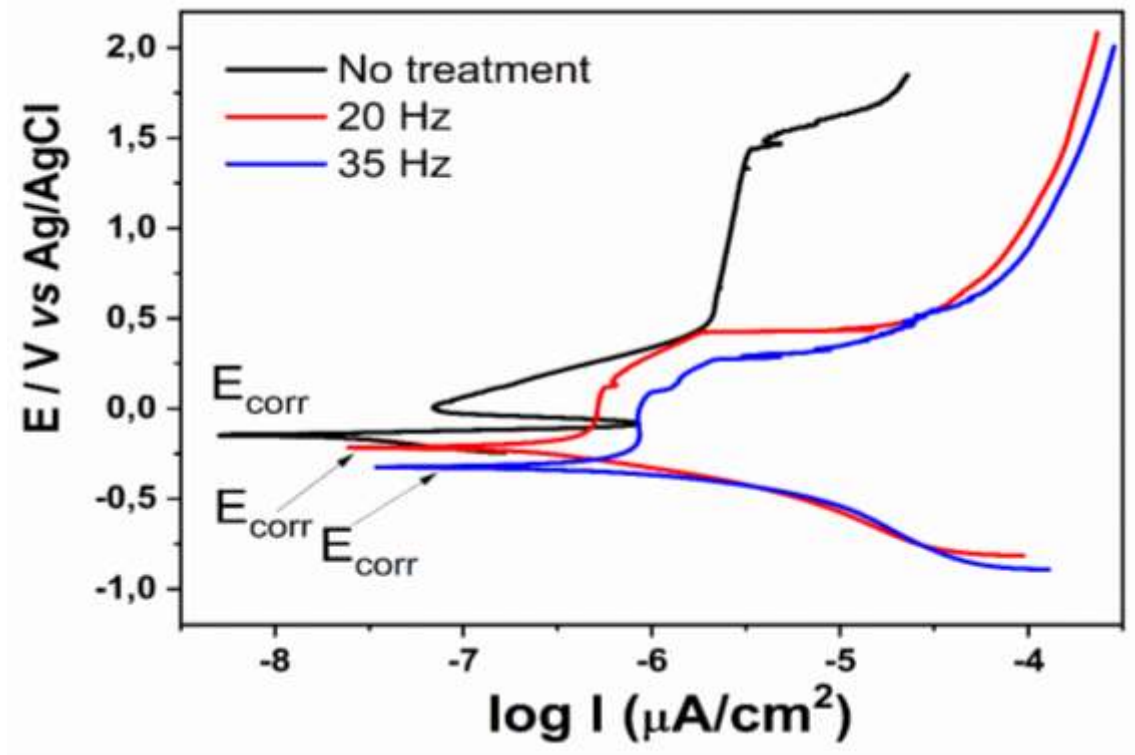
Source: Survey data.

### 3.2 Potentiodynamic polarization

The Figure 2 presents the curves obtained for the Ti-35Nb-7Zr-5Ta alloy with surface treatment to laser beam to the 20 Hz. A corrosion potential ( $E_{\text{corr}}$ ) of - 0.15 V (Ag / AgCl<sub>sat</sub>) was observed in the specimen polarization curve without surface treatment. Immediately after the corrosion potential, there is a sudden increase in the current density indicating the corrosion of the material. However, at -0.08 V (Ag / AgCl<sub>sat</sub>) it is possible to observe a repassivation of the surface and a decrease in the current density by an order of magnitude. Between 0.017 V (Ag / AgCl<sub>sat</sub>) and 0.48 V (Ag / AgCl<sub>sat</sub>) there is a gradual increase in the current density attributed to a new surface corrosion process. Between 0.5 V (Ag / AgCl<sub>sat</sub>) and 1.45 V (Ag / AgCl<sub>sat</sub>) a passivation zone is observed where there is no change in the current density value. After 1.5 V (Ag / AgCl<sub>sat</sub>) there is a sudden increase in the current density value attributed to the dissolution of passive protective layers occur in high overpotentials attributed to the dissolution of passive protective layers occur in high overpotentials a corrosion potential of - 0.22 V (Ag / AgCl<sub>sat</sub>) (frequency of 20 Hz) and -0.32 V (Ag / AgCl<sub>sat</sub>) (frequency of 35 Hz) was observed. The profile of the curves of the specimens in which the laser surface treatment took place, was vastly different from the untreated specimens, which makes clear the influence of the laser treatment on the surfaces of the metal alloys.

For the specimens treated with 20 Hz after the corrosion potential ( $E_{\text{corr}}$ ), there was an activation zone between - 0.14 V (Ag / AgCl<sub>sat</sub>) and 0.49 V (Ag / AgCl<sub>sat</sub>) where the current density increases slowly with the potential increase. After 0.5 V (Ag / AgCl<sub>sat</sub>) there is an abrupt increase in the corrosion density, probably due to the dissolution of the protective oxide layers or attack of chloride ions on the surface. For specimens irradiated by laser beam at a frequency of 35Hz, the active zone was between -0.25 V (Ag / AgCl<sub>sat</sub>) and 0.27 V (Ag / AgCl<sub>sat</sub>), where a gradual increase in current density is observed. After 0.29 V (Ag / AgCl<sub>sat</sub>) there is an increase in current density attributed to the dissolution of oxide layers or the diffusion of electrolyte to the surface of the metal alloy.

**Figure 2** - Potentiodynamic polarization curves for the Ti-35Nb-7Zr-5Ta alloy in 0.9% NaCl solution, in conditions without surface treatment and with laser beam irradiation at 20Hz and 35Hz.



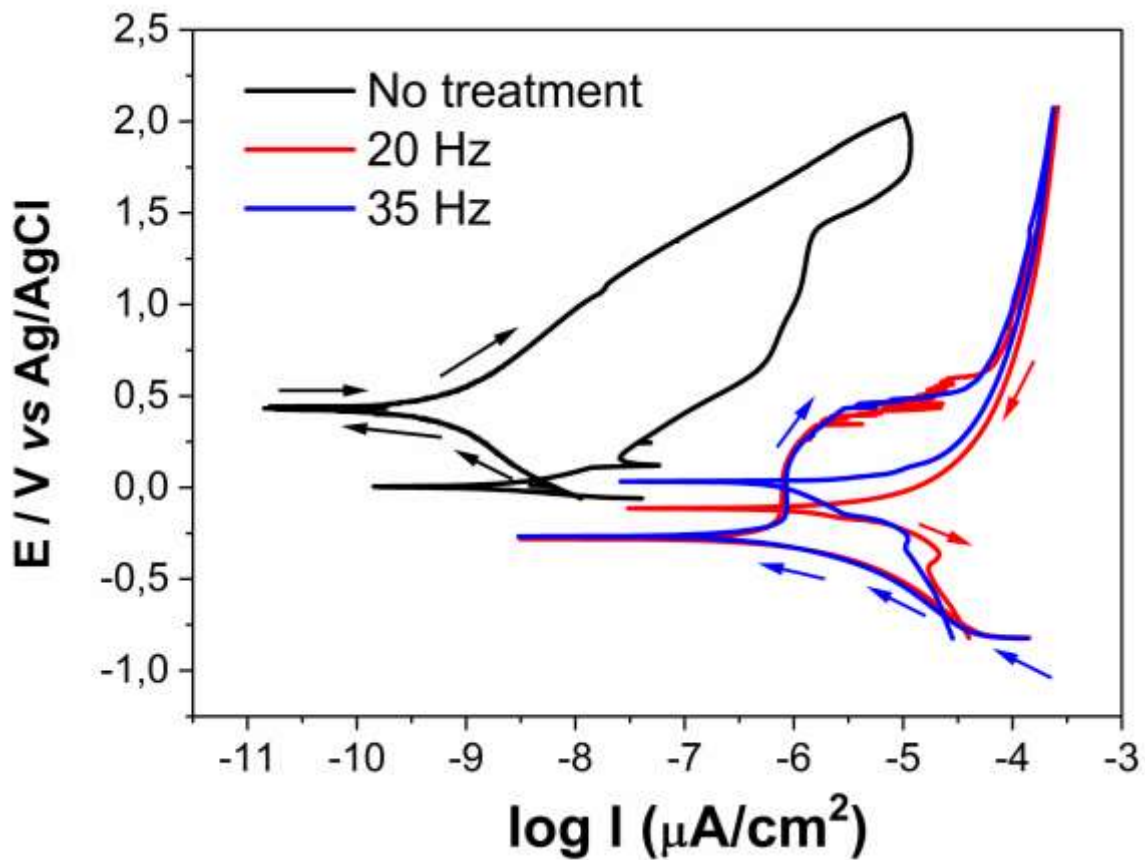
Source: Survey data.

### 3.3 Cyclic Polarization

In Figure 3 can observed the cyclic polarization curves, obtained for the specimen Ti-35Nb-7Zr-Ta alloy with surface treatment to laser beam to 35Hz. For the untreated specimen, the current density in the reverse scan was higher than in the direct scan. This indicates an increase in the active area of the electrode due to the formation of pits during direct scanning and shows this specimen has a lower corrosion resistance than the others. The corrosion potential of the cyclic polarization measures for the untreated specimen was greater than the corrosion potential obtained in the potentiodynamic polarization, which can be attributed to anodic sweeping before cyclic polarization can modify the metal surface.

For laser-treated specimens, the current density increases during the direct scan, but remains in the same order of magnitude in the reverse scan, which suggests corrosion products or oxides are formed and deposited on the surface blocking the anodic areas and points of contact. The cyclic polarization curves showed a higher repassivation potential for the laser-treated specimens in relation to the corrosion potential. This indicates improvements in the corrosion properties of the metal alloy when treated with laser. There was no passivation in any of the specimen at potentials up to 2 V (Ag / AgCl<sub>sat</sub>).

**Figure 3** - Cyclic polarization curves for the Ti-35Nb-7Zr-5Ta alloy in 0.9% NaCl solution, in conditions without surface treatment and with laser beam irradiation at 20Hz and 35Hz.



Source: Survey data.

#### 4. Discussion

The Ti-35Nb-7Zr-5Ta quaternary metal alloy, the material of choice for this study, presents characteristics favorable to the requirements of a biomaterial. Aiming at this, measures of evaluation of corrosion potential by means of electrochemical tests in specimen without surface modification and in specimen modified by laser beam. Methods for modifying the surfaces of implantable biomedical devices favor the protection of the biomaterial, as well as the osseointegration process, in this case positively influencing aspects such as: roughness, wettability, increased surface energy, which can bring improvements in the cellular response.

The dissolution process of the alloy metals is further accelerated by the presence of chloride ions in the physiological solution. Because of the adsorption of Cl<sup>-</sup> ions on the surface, the oxide stability decreases and the susceptibility to localized corrosion of the Ti-35Nb-7Zr-5Ta alloy increases.(Metikoš-Huković et al., 2003; Tanase et al., 2019)

In the corrosion tests the specimen analyzed in the three proposed conditions showed a continuous growth of the oxide film layer, although the specimen in the two proposed conditions of surface treatment by means of laser beam irradiation have shown a similar behavior in relation to formation of the Ti oxide film and resistance to corrosion, we were able to evaluate the group of specimen irradiated at 35 Hz, presented better characteristics for having formed a thicker and more compact oxide film on the surface, which increased the potential of repassivation in relation to the corrosion potential, indicating better performance in terms of corrosion properties.

The corrosion potentials determined from the polarization curve are lower than those obtained in open circuit potential measurements. This is expected as the polarization test was initiated at a cathodic potential in relation to the corrosion potential, so the passive film on the surface was at least partially removed due to the reduction to initial potentials.

## 5. Conclusion

The electrochemical techniques used in this investigation led to the following conclusions:

- Low density corrosion current was obtained for the titanium alloy tested in the 0.9% NaCl solution, showing it is a passive material in this electrolyte, which suggests good resistance to corrosion.
- The presence of the oxide film formed on the surface of the alloy characterizes a protection of the material against the aggressiveness of the medium, preventing the degradation of this material, thus avoiding possible contamination of the organism by metal ions.
- Electrochemical analyzes were presented as a powerful tool to evaluate and monitor the behavior of the  $\beta$ -Ti-35Nb-7Zr-5Ta alloy, allowing to detect small variations in the behavior and corrosion resistance of passive materials, such as titanium alloys.
- Corroborating with data from the literature, this work demonstrated the efficiency of laser surface modifications in  $\beta$  titanium alloys, attributing better passivation of the oxide film, which favors biomaterial protection, as well as in the osseointegration process.
- The authors suggest further studies to investigate the real composition of the oxide film formed on the Ti-35Nb-7Zr-5Ta alloy using techniques such as X-ray excited photoelectron spectroscopy (XPS), in addition to the complementary study of corrosion resistance by spectroscopy. electrochemical impedance (EIS), using the same parameters, as well as biocompatibility studies.

## References

- Capellato, P. et al. (2020). Avaliação da biocompatibilidade do polímero PCL recobrando a liga Ti-30Ta. *Research, Society and Development*, 9(8). <https://doi.org/http://dx.doi.org/10.33448/rsd-v9i8.5953>
- Chai, Y. W., Kim, H. Y., Hosoda, H., & Miyazaki, S. (2008). Interfacial defects in Ti-Nb shape memory alloys. *Acta Materialia*, 56(13), 3088–3097. <https://doi.org/10.1016/j.actamat.2008.02.045>
- Chen, J., Rungsiyakull, C., Li, W., Chen, Y., Swain, M., & Li, Q. (2013). Multiscale design of surface morphological gradient for osseointegration. *Journal of the Mechanical Behavior of Biomedical Materials*, 20, 387–397. <https://doi.org/10.1016/j.jmbbm.2012.08.019>
- De Assis, S. L., Wolyneć, S., & Costa, I. (2006). Corrosion characterization of titanium alloys by electrochemical techniques. *Electrochimica Acta*, 51(8–9), 1815–1819. <https://doi.org/10.1016/j.electacta.2005.02.121>
- Filho, E. D. A., Fraga, A. F., Bini, R. A., & Guastaldi, A. C. (2011). Bioactive coating on titanium implants modified by Nd:YVO 4 laser. *Applied Surface Science*, 257(10), 4575–4580. <https://doi.org/10.1016/j.apsusc.2010.12.056>
- Geetha, M., Singh, A. K., Asokamani, R., & Gogia, A. K. (2009). Ti based biomaterials, the ultimate choice for orthopaedic implants - A review. *Progress in Materials Science*, 54(3), 397–425. <https://doi.org/10.1016/j.pmatsci.2008.06.004>
- Kuroda, D., Niinomi, M., Morinaga, M., Kato, Y., & Yashiro, T. (1998). Design and mechanical properties of new  $\beta$  type titanium alloys for implant materials. *Materials Science and Engineering A*, 243(1–2), 244–249. [https://doi.org/10.1016/s0921-5093\(97\)00808-3](https://doi.org/10.1016/s0921-5093(97)00808-3)
- Kuroda, P. A. B., & Nascimento, M V.; & Grandini, C. R. (2020). Preparação e caracterização de uma liga de titânio com a adição de tântalo e zircônio para aplicações biomédicas Preparation and characterization of a titanium alloy with the addition of tantalum and zirconium for biomedical applications. *Revista Materia*, 25(2). <https://doi.org/10.1590/s1517-707620200002.1041>
- Laurindo, C. A. H.; Lepienski, C. A.; Amorim, F. L.; Torres, R. D.; & Soares, P. (2018). Mechanical and Tribological Properties of Ca/P-Doped Titanium Dioxide Layer Produced by Plasma Electrolytic Oxidation: Effects of Applied Voltage and Heat Treatment. *Tribology Transactions*, 61(4), 733–741. <https://doi.org/https://doi.org/10.1080/10402004.2017.1404176>
- Lopes, C. S., Donato, M., & Ramgi, P. (2016). Comparative corrosion behavior of titanium alloys (ti-15mo and ti-6al-4v) for dental implants applications: A review. *Corrosão e Proteção de Materiais*, 35(2), 05–14. <https://doi.org/10.19228/j.cpm.2016.35.04>



- López, M. F., Gutiérrez, A., & Jiménez, J. A. (2001). Surface characterization of new non-toxic titanium alloys for use as biomaterials. *Surface Science*, 482–485(PART 1), 300–305. [https://doi.org/10.1016/S0039-6028\(00\)01005-0](https://doi.org/10.1016/S0039-6028(00)01005-0)
- Metikoš-Huković, M., Kwokal, A., & Piljac, J. (2003). The influence of niobium and vanadium on passivity of titanium-based implants in physiological solution. *Biomaterials*, 24(21), 3765–3775. [https://doi.org/10.1016/S0142-9612\(03\)00252-7](https://doi.org/10.1016/S0142-9612(03)00252-7)
- Miotto, L. N., Fais, L. M. G., Ribeiro, A. L. R., & Vaz, L. G. (2016). Surface properties of Ti-35Nb-7Zr-5Ta: Effects of long-term immersion in artificial saliva and fluoride solution. *Journal of Prosthetic Dentistry*, 116(1), 102–111. <https://doi.org/10.1016/j.prosdent.2015.10.024>
- Mish, C. E. (2000). *Implantes Dentais Contemporâneos*. Pancast.
- Mohammed, M. T., Khan, Z. A., Geetha, M., & Siddiquee, A. N. (2015). Microstructure, mechanical properties and electrochemical behavior of a novel biomedical titanium alloy subjected to thermo-mechanical processing including aging. *Journal of Alloys and Compounds*, 634, 272–280. <https://doi.org/10.1016/j.jallcom.2015.02.095>
- Niinomi, M.; Kuroda, D.; Fukunaga, K. I.; Morinaga, M.; Kato, Y.; Yashiro, T.; & Suzuki, A. (1999). Corrosion wear fracture of new b type biomedical titanium alloys. *Materials Science and Engineering A*, 263(2), 193–199. [https://doi.org/10.1016/S0921-5093\(98\)01167-8](https://doi.org/10.1016/S0921-5093(98)01167-8)
- Paital, S. R., & Dahotre, N. B. (2009). Calcium phosphate coatings for bio-implant applications: Materials, performance factors, and methodologies. *Materials Science and Engineering R: Reports*, 66(1–3), 1–70. <https://doi.org/10.1016/j.mser.2009.05.001>
- Queiroz, T. P., Souza, F. Á., Guastaldi, A. C., Margonar, R., Garcia-Júnior, I. R., & Hochuli-Vieira, E. (2013). Commercially pure titanium implants with surfaces modified by laser beam with and without chemical deposition of apatite. Biomechanical and topographical analysis in rabbits. *Clinical Oral Implants Research*, 24(8), 896–903. <https://doi.org/10.1111/j.1600-0501.2012.02471.x>
- Rodrigues, A. V., Oliveira, N. T. C., dos Santos, M. L., & Guastaldi, A. C. (2015). Electrochemical behavior and corrosion resistance of Ti–15Mo alloy in naturally-aerated solutions, containing chloride and fluoride ions. *Journal of Materials Science: Materials in Medicine*, 26(1), 1–9. <https://doi.org/10.1007/s10856-014-5323-0>
- Rungsiyakull, C., Li, Q., Sun, G., Li, W., & Swain, M. V. (2010). Surface morphology optimization for osseointegration of coated implants. *Biomaterials*, 31(27), 7196–7204. <https://doi.org/10.1016/j.biomaterials.2010.05.077>
- Santos, L. D. B., Maria, T., Freire, V., Sampaio, N. D. M., & Oliveira, A. S. de. (2007). *Aspectos biomecânicos das próteses sobre im- plantes Biomechanics aspects of the implant-supported pros- theses*. 6(1), 13–18.
- Silva, F. S. d., Bedoya, J., Dosta, S., Cinca, N., Cano, I. G., Guilemany, J. M., & Benedetti, A. V. (2017). Corrosion characteristics of cold gas spray coatings of reinforced aluminum deposited onto carbon steel. *Corrosion Science*, 114, 57–71. <https://doi.org/10.1016/j.corsci.2016.10.019>
- Tanase, C. E., Golozar, M., Best, S. M., & Brooks, R. A. (2019). Cell response to plasma electrolytic oxidation surface-modified low-modulus  $\beta$ -type titanium alloys. *Colloids and Surfaces B: Biointerfaces*, 176, 176–184. <https://doi.org/10.1016/j.colsurfb.2018.12.064>
- Trivinho-Strixino, F; Santos, J S; & Sikora, M. S. (2017). Electrochemical Synthesis of Nanostructured Materials. *Nanostructures*, 53–103. <https://doi.org/https://doi.org/10.1016/B978-0-323-49782-4.00003-6>
- Valente, C. B. M. (2017). *Estudo do Comportamento Mecânico de uma Liga de Titânio-Tântalo, Ti10Ta, Produzida por LASER Cladding* [Universidade Nova de Lisboa]. <http://hdl.handle.net/10362/27686>
- Varella Rodrigues, A., & Carlos Guastaldi, A. (2018). Ti-Mo alloys: corrosion study in solutions simulating commercial gels. *Journal of Polymer Science and Engineering*, 1(4), 1–7. <https://doi.org/10.24294/jpse.v1i4.897>